Plasmonic light trapping in nanostructured metal surfaces

A. Polyakov,[1,a)] S. Cabrini,[2] S. Dhuey,[2] B. Harteneck,[2] P. J. Schuck,[2] and H. A. Padmore[1]
[1]*LBNL, 1 Cyclotron Road, Berkeley, California 94720, USA*
[2]*Molecular Foundry, LBNL, 1 Cyclotron Road, Berkeley, California 94720, USA*

(Received 6 February 2011; accepted 28 April 2011; published online 17 May 2011)

We demonstrate the plasmonic trapping of light in nanometer sized trenches etched into in a planar metal surface. The subwavelength grating structure is shown to efficiently couple to p-polarized light and can be designed to achieve complete absorption at any desired wavelength from the UV to the IR. These structures have a number of useful practical features such as high polarization sensitivity, omnidirectional absorption and extreme field concentration. © *2011 American Institute of Physics*. [doi:10.1063/1.3592567]

Metals are commonly used as ultrafast photoemitters for free-electron lasers[1] and as field concentrators for generation of harmonics in a laser-driven plasma.[2] In these applications high optical reflectivity is problematic. This is especially true of gold (Au), silver (Ag), and aluminum (Al), which are all efficient reflectors due to their free-electronlike behavior. However, by collective excitation of electrons in the form of a plasmon, free-electron metals can completely absorb light. The key to this process is to make up the missing momentum between light and the plasmon by some means. This can be done by passing light through a prism on which the metal is deposited or by making a corrugated metal surface that acts as a grating.[3] These methods, however, are not applicable to many experimental methods: for example, those involving high peak current or high gradient fields. Here, we demonstrate a practical realization of a method recently proposed theoretically where light is converted into plasmons, which are trapped in nanotrenches[4] and dissipated in the metal. For some applications this type of coupling is advantageous due to the extremely large field enhancement and will be a powerful tool in ultrafast photocathode applications using multiphoton photoemission[1] and laser harmonic generation.[2]

The approach is to pattern the metal surface with a subwavelength grating composed of rectangular trenches of a defined depth h and width w, on a period p as shown in Fig. 1. The period p is always less than the wavelength at which a plasmon resonance is required. Light couples from the flat surface into the trenches and is converted to plasmons at the sharp edges of the trench, which contain all the Fourier frequencies required for momentum matching. The plasmons that propagate down the trench walls can be described in the framework of surface plasmon polariton traveling within the metal insulator metal (MIM) waveguide and the plasmon dispersion relation can be found directly from solution of the Maxwell equations.[5]

As illustrated in Fig. 2, by use of a few nanometer widths, very large wave vectors can be supported in the MIM waveguide. Closing one end of the MIM waveguide at a distance h results in the tunable resonant cavities as in Fig. 1. In this case, the depth of the cavity can be adjusted so that plasmons traveling from the top surface interfere destructively with plasmons reflected from the bottom of the cavity, resulting in complete absorption. The cumulative reflectivity response is, however, a combination of the individual nanotrench responses with the collective interaction of adjacent periods. This picture is more complex and optimal design of the system requires the use of finite difference time domain (FDTD) modeling.

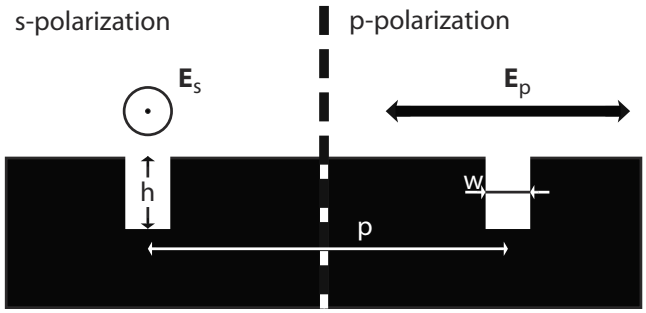

FIG. 1. The polarization is defined in reference to the orientation of the nanotrenches.

Figure 3 shows the simulations results for Au, where the dimensions of the nanotrenches were adjusted to produce essentially 100% absorption at the target wavelength. This resonance wavelength can be readily adjusted throughout the

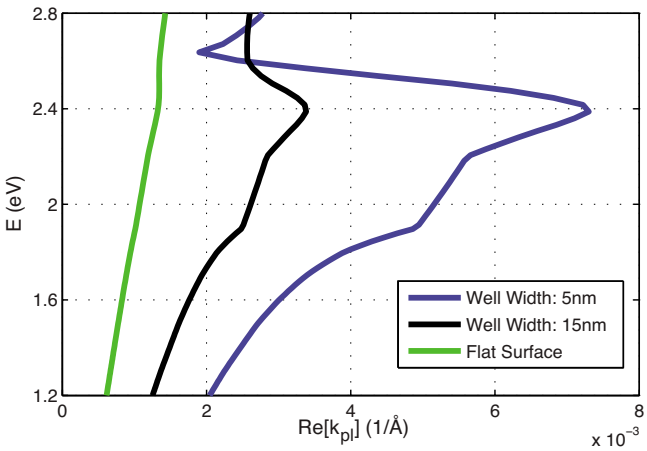

FIG. 2. (Color online) The dispersion relation, calculated from the metal-insulator-metal model using interpolated optical constants from Ref. 6, shows large wave vectors accessible in very narrow trenches.

[a)]Electronic mail: apolyakov@berkeley.edu. AS&T Graduate Group, University of California Berkeley.

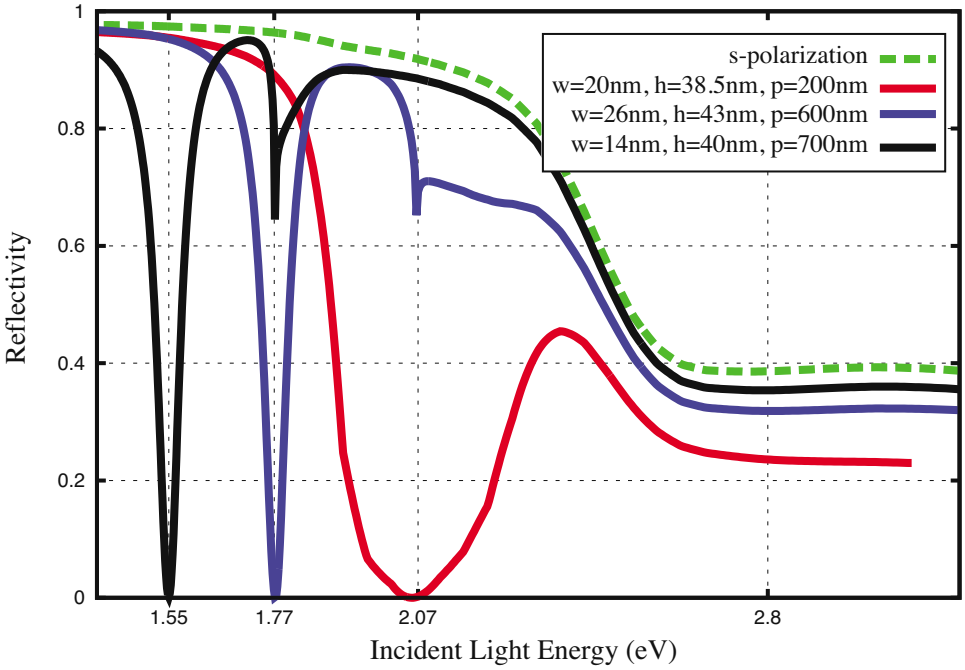

FIG. 3. (Color online) Complete absorption in aluminum and gold nanotrenches tuned for conventional laser wavelengths. The dimensions were calculated using RCWA code and verified using FDTD methods (see Refs. 7 and 8). Note that the minor reflectivity dips corresponding to the grating plasmon (due to the periodicity of the nanotrenches) are clearly visible in gold. The s-polarized reflectivity response is equivalent to that of a flat surface metal.

ultraviolet (UV), visible, and IR ranges. It should be noted that an important characteristic of these devices is the omnidirectionality of the absorption and the high selectivity between s- and p-polarized light.

The FDTD simulations can also be used to extract the field enhancement caused by the concentration of the fields into the nanocavity. One example is shown in Fig. 4, where field enhancement of a few hundred can be readily achieved, in good agreement with the previous calculations by Zhang *et al.*[9] Note the lack of any field enhancement for the s-polarized light. The field enhancement can be used in many applications, but of concern here is the multiphoton photoemission from metallic photocathodes, where local emission scales as the *n*th power of the electric field strength for an *n*th order photoemission process.

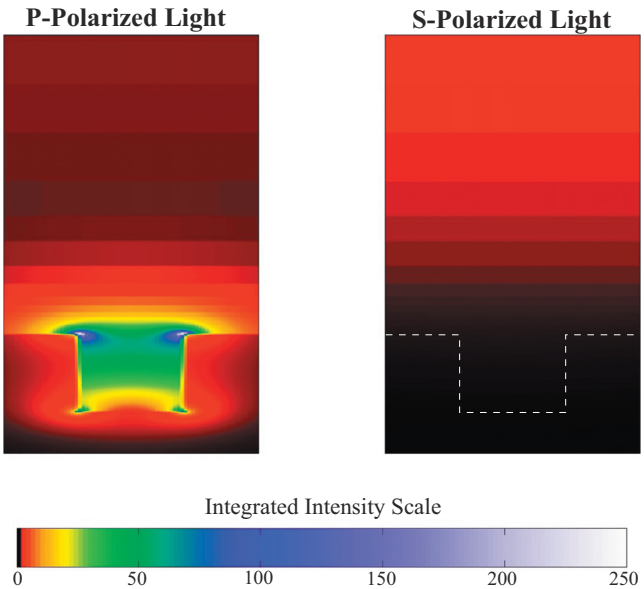

FIG. 4. (Color) Field enhancement for a nanotrench with $w=15$ nm, $h=31$ nm, and $p=200$ nm in gold. The comparison between s- and p-polarized light at 600 nm shows the extreme polarization selectivity of the nanotrenches.

In order to demonstrate these properties, we have fabricated nanotrench structures in gold and measured their optical properties. The fabrication process is illustrated in Figs. 5(a)–5(c). The silicon (110) wafer was used as a substrate for the template made by electron beam lithography on the hydrogen silsesquioxane (HSQ) resist. Gold was evaporated on the template and a glass plate was epoxied to the whole structure for support. The resulting structure was then submerged in potassium hydroxide solution separating the gold-on-glass sample from the template. A 4 mm^2 area on the gold surface was patterned with nanotrenches forming dashed lines as illustrated in the Fig. 6 (top inset). The sample cross section is shown in Fig. 5(d).

Figure 6 shows the reflectivity over the spectral region of the absorption. The figure also shows the results of a FDTD simulation using the measured average trench shape as input: 18 nm wide by 30 nm deep and slightly rounded at the upper surface and the bottom. The optical reflectivity of the patterned area was measured using an imaging technique, where light from a broadband light source was collimated

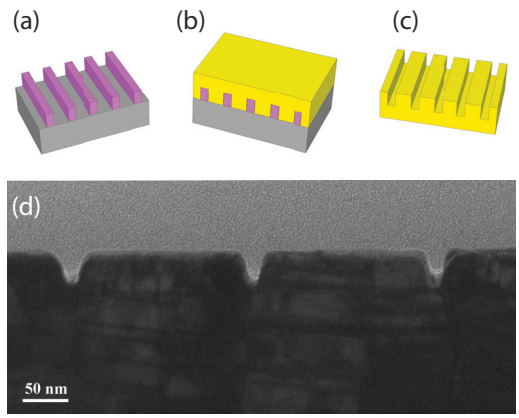

FIG. 5. (Color) The nanolithography steps are: (a) the e-beam resist, HSQ, is patterned on the silicon substrate creating a template, (b) the gold is evaporated onto the template, and (c) the template is removed in the KOH bath. The cross section of the resulting structure is shown in (d).

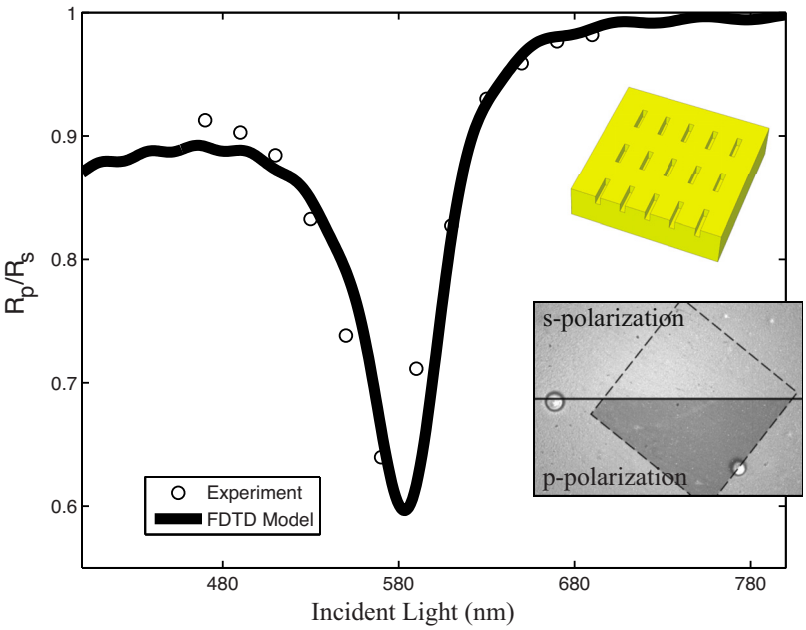

FIG. 6. (Color online) Reflectivity of a nanotrench surface. R_p/R_s is the ratio of the reflectivity with the E vector perpendicular and parallel to the trenches. The dots show data and the solid line shows the results of a FDTD simulation, using the measured average shape of the trenches; the top inset shows the dashed geometry of the nanotrenches. The bottom inset shows a reflectivity image of the patterned sample with light polarized parallel (top half) and perpendicular (bottom half) to the trenches; the dashed lines outline the total patterned area.

and reflected from the metal surface at near-normal incidence. Due to the omnidirectionality of light-trapping a deviation of $\pm 30°$ away from the normal produced no significant difference in the reflectivity response. The incident light source was monochromatized using a UV-visible monochromator and the reflected light was detected by a charge coupled device camera. The system, therefore, images the reflectivity over a field larger than the nanostructured area. A composite image showing the s- and p-polarized reflectivity response at the absorption peak is shown in Fig. 6 (bottom inset).

The data in Fig. 6 are presented as R_p/R_s: the ratio between reflectivity with the electric vector of light perpendicular and parallel to the trenches, see Fig. 1. For a structure as in Fig. 5(c), R_p/R_s should be zero at the absorption maximum. Due to the restrictions of the lithography used, the trenches were designed to have a *fill-factor* of 0.5 forming dashed lines as illustrated in Fig. 6 (top inset) instead of continuous ones as in Fig. 5(c). Therefore, we expected the reflectivity dip to reach 0.5 compared to the measured 0.6, which corresponds to eight times increase in absorption over the plain gold surface (5% absorption at 580 nm). For continuous lines this would be a factor of 16 compared to the maximum of 20 for a perfect structure or 80% absorption efficiency. The slanted walls and the nonoptimal edge profile, as seen in the cross section measurements in Fig. 5(d), all contributed to the reduced absorption efficiency of the sample. An improved lithographic process is now being used that has produced higher quality continuous lines, and so, given the excellent agreement between the experimental measurements and the FDTD model, as shown in Fig. 6, R_p/R_s values approaching zero can be expected.

In summary, we have shown that nanotrenches in a metallic surface can strongly couple to light and can induce complete absorption. This phenomenon has many practical applications from ultrafast metallic photocathodes and generation of laser harmonics through field concentration to polarization control and switching.

Portions of this work were performed as a User project at the Molecular Foundry, Lawrence Berkeley National Laboratory, which is supported by the Office of Science, Office of Basic Energy Sciences, of the U.S. Department of Energy under Contract No. DE-AC0205CH11231.

[1]P. Musumeci, L. Cultrera, M. Ferrario, D. Filippetto, G. Gatti, M. Gutierrez, J. Moody, N. Moore, J. Rosenzweig, C. Scoby, G. Travish, and C. Vicario, Phys. Rev. Lett. **104**, 084801 (2010).
[2]S. Kim, J. Jin, Y.-J. Kim, I.-Y. Park, Y. Kim, and S.-W. Kim, Nature (London) **453**, 757 (2008).
[3]H. Raether, *Surface Plasmons on Smooth and Rough Surfaces and on Gratings* (Springer, Berlin, 1988).
[4]J. Le Perchec, P. Quemerais, A. Barbara, and T. Lopez-Rios, Phys. Rev. Lett. **100**, 066408 (2008).
[5]J. Dionne, L. Sweatlock, H. Atwater, and A. Polman, Phys. Rev. B **72**, 075405 (2005).
[6]E. Palik, *Handbook of the Optical Constants of Solids* (Academic Press, New York, 1985), Vol. 1.
[7]D. Fluckiger, Grating solver, 2011 http://www.gsolver.com.
[8]Lumerical, Finite difference time domain solutions, 2011 http://www.lumerical.com.
[9]S. Zhang, H. Liu, and G. Mu, J. Opt. Soc. Am. A **27**, 1555 (2010).